Design of a neural network control scheme for the maximum power point tracking (MPPT)

M.S. Aït Cheikh, M. Haddadi and A. Zerguerras

Laboratoire des Dispositifs de Communication et de Conversion Photovoltaïque
Ecole Nationale Polytechnique
10, Avenue Hassen Badi, El Harrach, Alger

(reçu le 14 Octobre 2006 – accepté le 25 Mars 2007)

Abstract - *This paper proposes a control method for the maximum power point tracking (MPPT) of a photovoltaic system and this with the aim of increasing the output power of a photovoltaic system. An electronic controller is built-in between the photovoltaic generator and the load, whose principal role is the permanent monitoring of the maximum power point of the PV generator commonly called MPPT (Maximum Power Point Tracking) and that in general by acting on a DC-DC converter device. The contribution of this paper resides at the level DC converter device. The contribution of this paper resides at the level of the electric output of the converter, which can be estimated thru three state variables, which are the solar insolation, the temperature of the junction and information on the dynamics of the charging voltage if it exists.*

Résumé - *Cet article propose une méthode de poursuite du point de puissance maximale (MPPT) pour les systèmes photovoltaïques et cela dans le but d'augmenter le rendement en puissance d'un module PV ou d'un champ de modules PV. Un contrôleur électronique est incorporé entre le générateur PV et la charge, dont le rôle principal est la surveillance en permanence du point de puissance maximale du générateur PV appelé communément MPPT (Maximum Power Point Tracking) et cela en général par action sur un dispositif de conversion DC-DC. La contribution de cet article réside au niveau de la sortie en puissance électrique du convertisseur qui peut être estimé à partir de trois variables d'états que sont respectivement l'ensoleillement, la température de la jonction et une information sur la dynamique de la tension de charge si elle existe.*

Key words: Photovoltaic - Neural - MPPT - Converter.

1. INTRODUCTION

Since last century, consumption in energy increased in a considerable way. But our coal, oil or gas resources are not eternal. It is preferable not to burn them so that not to worsen pollution.

The solution consists of the use of renewable energies such as hydraulic, wind or solar power. The use of this type of energy increased by 12,5 % since 1990.

What is encouraging is the world demand for solar power supply systems which has increased constantly for the last 15 years. Today, the world photovoltaic industry rests primarily on the isolated areas needs for reliable and inexpensive power supply. In a great number of applications, the photovoltaic is one of the most profitable solutions. Among these applications, one can quote isolated feeding systems for country cottages or far away residences, navigation assistances for the coastal guard, water pumping in farms.

2. CONSTITUTION OF A PHOTOVOLTAIC GENERATOR

A solar cell is a semiconductor device which absorbs the light and converts it into electric power. The most common cell today is a simple PN silicon junction cell with approximately 17 % of efficiency.

When this cell is exposed to the radiations, the photons create pairs of electron - hole with energy larger than the energy band of the semiconductor $\left(h\nu > E_g\right)$. Taking into account the

photo current produced, I_{ph}, as well as the joule effect which results in losses of energy at the level of the series and parallel resistances R_S and R_P, enables us to model the behaviour of a photovoltaic cell. The voltage characteristic equation of a cell obtained in generating mode is the same as one of a module, with one more parameter which indicates the number of cells in series (Z). So the equation of the module is as follows [1-15]:

$$I = I_{ph} - I_{S1}\left(e^{\frac{q(V + IZR_P)}{Z\eta_1 KT}} - 1 \right) - I_{S2}\left(e^{\frac{q(V + IZR_S)}{Z\eta_2 KT}} - 1 \right) - \frac{V + IZR_S}{ZR_P} \qquad (1)$$

where: I_{ph} : Photocurrent produced; I_{S1} and I_{S2} : Diodes saturation current; η_1 and η_2 : Ideality diodes factors; R_S and R_P : Series and parallel resistance; T : Absolute temperature (K); Z : Number of cells in series forming the module.

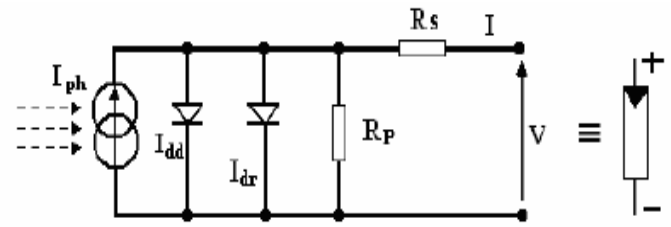

Fig. 1: Equivalent diagram deduced from equation (1) without parameter Z

In average, each cell can provide a continuous nominal voltage of 0,6 volts, thus to obtain a voltage higher than 12 volts it is necessary to put several cells in series. Figure 2 shows the module voltage and power behaviour with 36 identical cells.

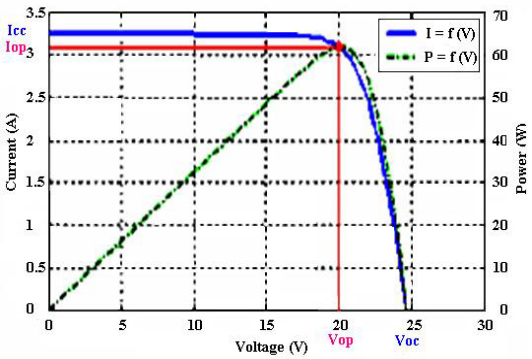

Fig. 2: Behaviour of a 36 identical cells module

From equation (1) we notice that the output current of the PV module depends on the photocurrent itself, which itself depends on the solar insolation and the junction temperature of the cells of the module, consequently the power which a module can deliver depends on the solar insolation and the temperature of the junction [16].

These dependencies are illustrated in figures 3 and 4, which respectively represent the influence of the solar insolation and the temperature of the junctions, which is supposed uniformly distributed over all the cells of the module, on the current output module versus the voltage module.

3. OPERATION OF A PV GENERATOR AT ITS MAXIMUM POWER

The global design of optimized photovoltaic system is rather difficult. Indeed, for a photovoltaic generator, the production of power strongly varies according to solar insolation, temperature, but also of the system ageing.

So, for a connection source-load to be possible, an operating point, corresponding to the intersection of the electric characteristics must exist.

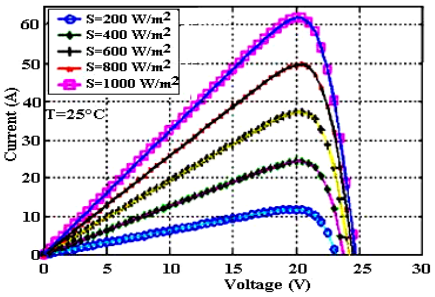

Fig. 3: Influence of the solar radiation

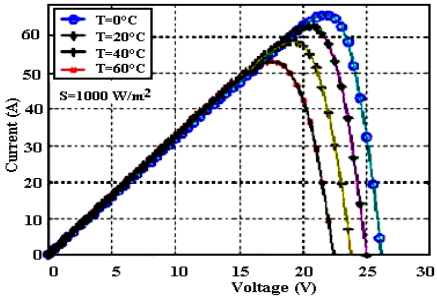

Fig. 4: Influence of the temperature of junction

To understand this, let us take for example the case of a direct connection between a PV generator and a battery (Fig. 5).

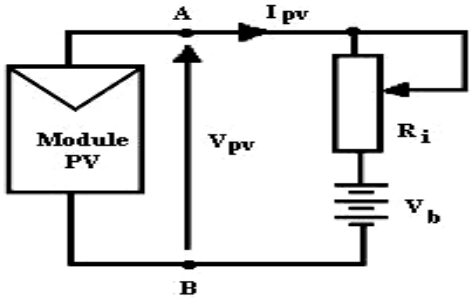

Fig. 5: Direct electric connection between a module and a battery.

The electrical characteristic which describes any possible configuration between PV Module-Battery is illustrated in figure 6.

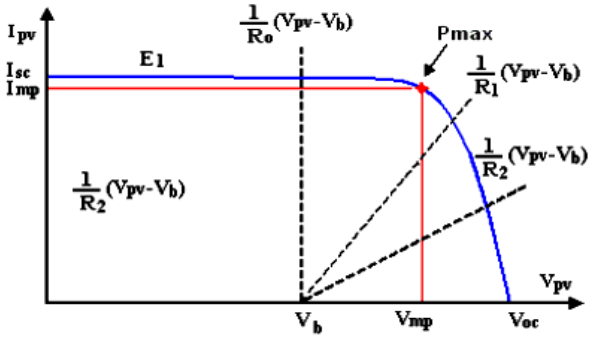

Fig. 6: Source-load characteristics

As we can note it in figure 6, the PV module operation strongly depends on the load characteristics (battery) to which it is associated. Indeed, for the battery, with internal resistance R_1, the optimal adaptation occurs only at one particular operating point, called Maximum Power Point (MPP) and noted in our case P_{max}. This curve corresponds to the power which a PV module, for a given curve $I(V)$, can deliver. For a load of battery type, the point of connection source-load is not optimal.

Thus, when a direct connection is carried out between the source and the load, the output of the unit is seldom maximum. To circumvent this problem, it is necessary to add an adaptation device between the source and the load, which generally is a Buck-Boost chopper, (Fig. 7), described by the equations (2), (3) and (4).

$$i_L = \frac{1}{d}\left(i - C_1 \frac{dV_i}{dt} \right) \tag{2}$$

$$i_0 = -(1-d) i_L - C_2 \frac{dV_0}{dt} \tag{3}$$

$$V_i = \frac{1}{d}\left(\frac{di_L}{dt} - (1-d) V_0 \right) \tag{4}$$

The parameter d indicates the width of impulse to the phase at the opening switch K (ON) over one period (ON/OFF) of the switch.

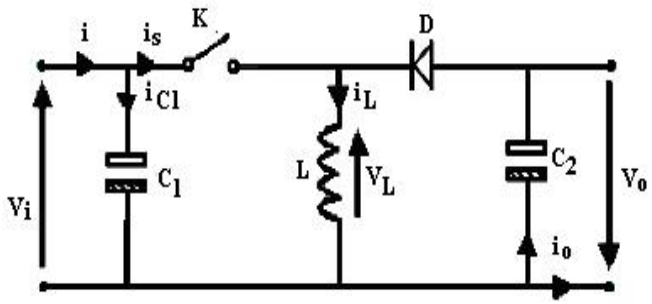

Fig. 7: Ideal circuit of the Buck-Boost chopper

In order to continuously locate the position of the MPP, the adaptation device must at every moment know the pulse width (ON) which is necessary to apply to the load to carry out the adaptation. This information is provided by another 'intelligent' element who must supervise in a continuous way dynamics of the maximum power point. Generally the intelligent element is an algorithm which allows the evaluation of the control signal according to some measured state variables which are the current and voltage output respectively I_{PV} and V_{PV}, through which the position of the MPP can be detected.

A significant number of algorithm have been elaborated since 1968, [17], among them perturbation and observation algorithm (P&O), improved P&O and incremental conductance (IncCond).

A simulation, using algorithm P&O for standard climatic conditions in temperature and solar insolation, which is illustrated in figure 8, clearly shows the delay recorded by the algorithm to reach the final MPP.

These methods are iterative based on the increase or the decrease value of the control variable according to a certain time period to be fixed arbitrarily. Each one of these methods present disadvantages such as precision and convergence slowness, which cause in one way or another losses in power.

In order to be able to reduce delay constraints loss in power, and increase precision in the control and output signals a new method which is not complex to realize has been tested. This is commonly known as the neural network method.

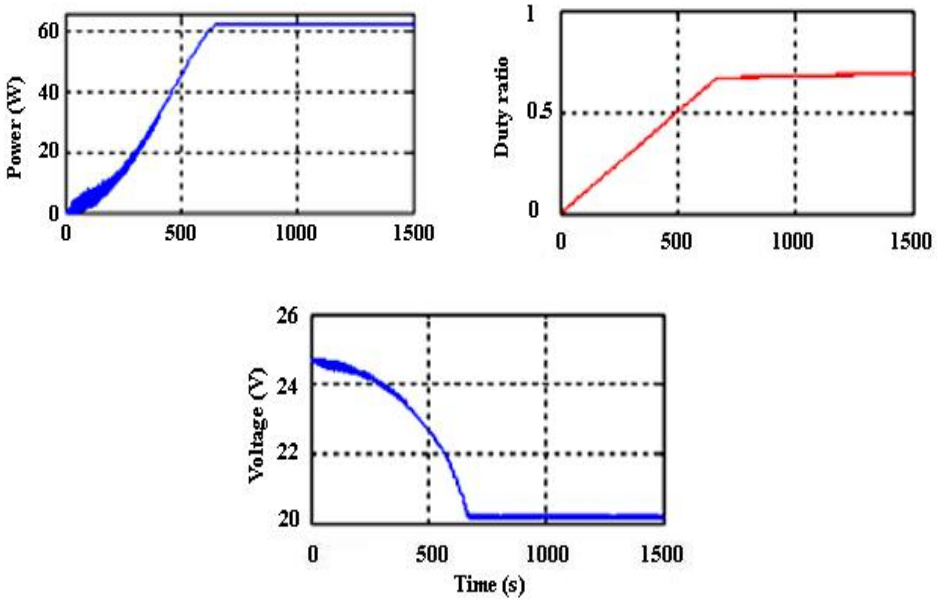

Fig. 8: Signals of power, control and PV voltage

4 NEURAL NETWORK AND PRINCIPLE OF OPERATION

A neuron is a cell made up of a cellular body and a core. The cellular body ramifies to form the dendrites. It is thru the dendrites that information to the neuron is conveyed towards the soma, body of the neuron [18].

The transmission between two neurons is not direct. In fact, there is an intercellular space of a few tens of Angstroms (10^9 m) between the axon of the related neuron and dendrites of the efferent neuron. The junction between two neurons is called the synapse, (Fig. 9), which works like a valve. It controls the flow rate of information. Since information about the function to be carried is stored at the level of all the synapses, it is necessary to parameterize all the synapses according to a suitable training or goal to be fulfilled.

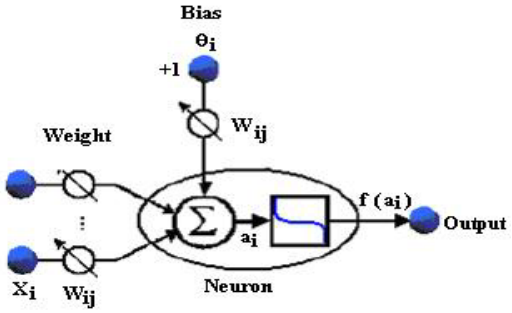

Fig. 9: Representation of an artificial neuron

The behaviour of a neuron is divided into two phases. First of all is usually the calculation of the balanced sum a_i of the entries, where neuron I receives signals of N neurons according to the following expression:

$$a_i = \sum_{j=1}^{N} W_{ij} \times x_j \tag{5}$$

The states variables x_i are evaluated by activation functions which generally limit the output of the neurons.

$$x_i = f(a_i) \tag{6}$$

The activation function used is the sigmoid function defined as follow:

$$x_i = \frac{\exp(a_i) - 1}{\exp(a_i) + 1} \tag{7}$$

Connections between the neurons, which make the network, describe the topology of the model. It can be unspecified, but generally it is the multi-layer (Fig. 10) which used also in this work.

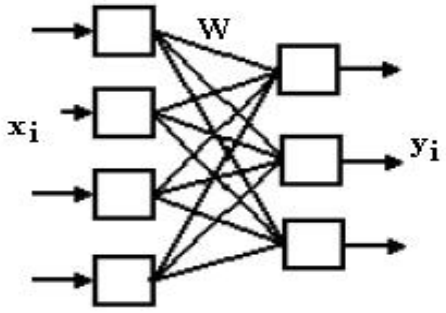

Fig. 10: Structure of a multi-layer network

The learning stage of the network is performed by updating the weights and biases using the backpropagation algorithm with the gradient-descent method in order to minimize a mean-squared-error performance index given as:

$$J = \frac{1}{2} \sum_{K=1}^{N_2} \left(y_i^{des} - y_i \right)^2 \tag{8}$$

With:

y_i^{des} : the i-th desired output of the system

y_i : the i-th computed output of the system

N_2 : The number neurons.

The problem consists in determining the weights W of all the layers which minimize the performance criterion J [19].

The update of W is done according to the following rule:

$$\Delta W = -\eta \frac{\partial J}{\partial W} \tag{9}$$

$$W_{ij}^{(k)}(t+1) = W_{ij}^{(k)}(t) - \Delta W \tag{10}$$

In fact this shows the variations of J with regard to the variations of the weights. Equation (9) is solved according to following the gradient algorithm:

- Output layer

  Where N_2 is the number of neurons in the layer K (output layer), N_1 the number of neurons in the layer $(K-1)$ (the last hidden layer).

$$\frac{\partial J}{\partial W_{ij}^{(k)}} = \frac{\partial J}{\partial y_i^{(k)}} \frac{\partial y_i^{(k)}}{\partial a_i^{(k)}} \frac{\partial a_i^{(k)}}{\partial W_{ij}^{(k)}} \tag{11}$$

- Hidden layers

  Where N_0 is the number of neurons of the layer $(K-2)$.

$$\frac{\partial J}{\partial W_{ji}^{(k-1)}} = \frac{\partial J}{\partial X_j^{(k-1)}} \frac{\partial X_j^{(k-1)}}{\partial a_j^{(k)}} \frac{\partial a_j^{(k-1)}}{\partial W_{ji}^{(k-1)}} \tag{12}$$

5. APPLICATION AND SIMULATION

Thru this method, which differs from the others, we show that we do not need any more measurements of the current and the voltage module to evaluate the output power and thus, to detect the position of the PPM. The consideration of direct effect state variables (solar insolation, junction temperature and dynamics of the charging voltage (case of a battery)) enabled to lead us to the synthesis of a neural network method

Figure 11 shows us the bloc diagrams of that structure.

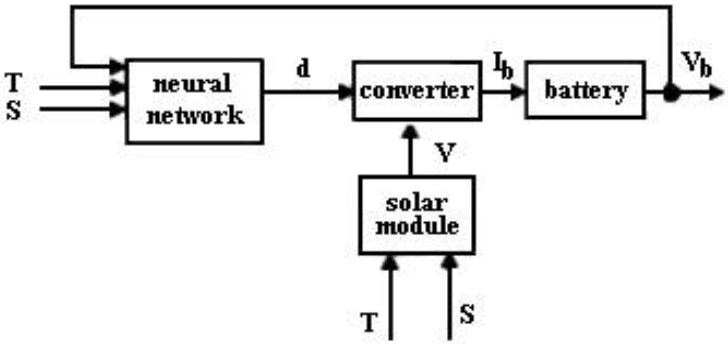

Fig. 11: Neural Network control structure

While the neuronal structure of training of the controller is such as it is schematized on figure 12.

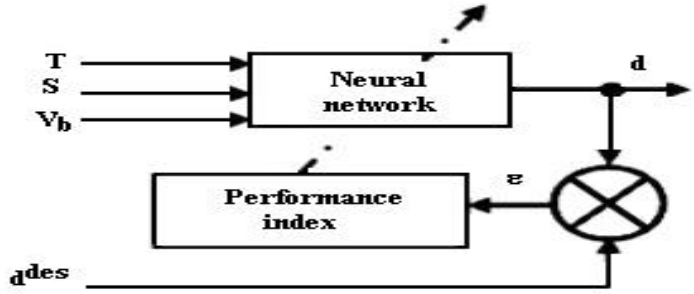

Fig. 12: Training of the neuronal controller

The training is carried out on a basis of data containing the following variables of states: (T : temperature of junction, S : solar insolation, V_b : battery dynamic voltage and D^{des} : desired cyclic duty ratio corresponding).

After having carried out the training stage of the network, it is inserted in the control architecture of figure 11. Afterwards it has been tested and its control performances, for the maximum power point tracking with random climatic condition changes in solar insolation and temperature, have been recorded.

The results obtained, illustrated in figure 13, are compared on the same figure with that of incremental of conductance, in order to be able to appreciate the improvements made by the neural network method.

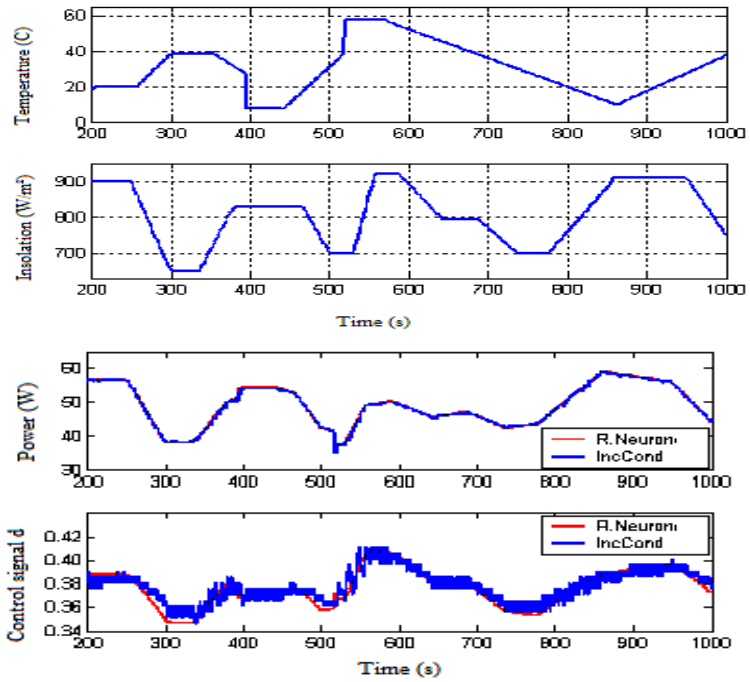

Fig. 13: Output power and control signals generated by the neuronal and incremental conductance method with a Buck-Boost chopper, for random temperature and solar insolation variations

The performance which presents the neuronal method over the incremental conductance method resides first of all in its speed to estimate the control signal corresponding to the position of the PPM without oscillations, and secondly, reaching the maximum power value deprived of all oscillations, and thirdly it is definitely higher than that obtained by the incremental method. All this is confirmed by figure 14.

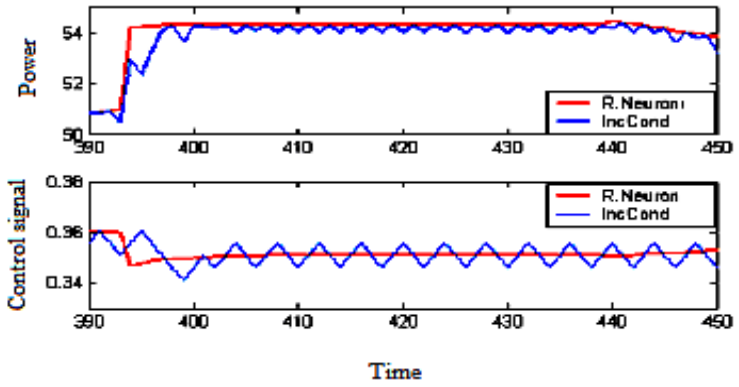

Fig. 14: Powers signals generated by neuronal controller and incremental conductance

It is also confirmed by figure 15 where we present the variation in power according to equation 13:

$$err = P_{rn} - P_{inc} \tag{13}$$

err : Variation in power

P_{rn} : Power given by the neuronal method

P_{inc} : Power given by the incremental method.

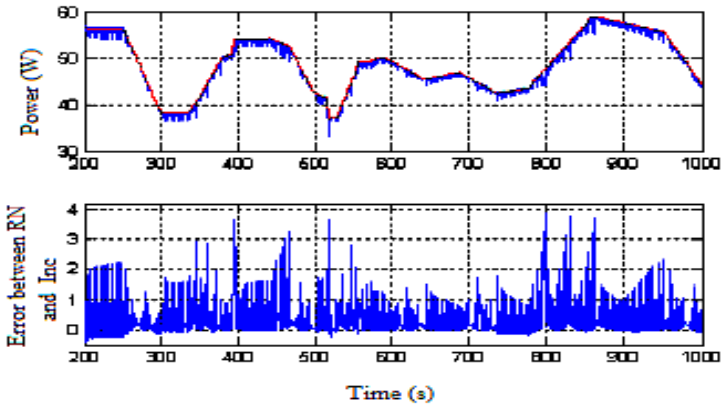

Fig. 15: Power for different solar insolation values

6. CONCLUSION

The goal of this work is to introduce the use of neural network in the power output control of a solar panel. It has been compared with another maximum power point tracking scheme and showed improvement in the power output value as well as in the time response.

The simulations carried out show that even under various atmospheric conditions the neuronal controller responded better than the other method used. This control method could let us think that it could be applied to complex and nonlinear systems and consolidate the idea that it may have better performances over other control scheme. This method reduces disadvantages which appear in the traditional methods.

REFERENCES

[1] T. Fromherz *et al.*, '*Energy MATER*', Cells Ground., pp. 61 – 63, 2000.

[2] S.E. Shaheen *et al.*, Appl. Phys. Lett, pp. 78 - 841. 2001.

[3] K. Takahashi *et al.*, 'Energy MATER', Cells Ground., pp. 63 – 403, 2000.

[4] D. Meissner, Photon, pp. 2 – 34, 1999.

[5] M.A. Green, '*Silicon Solar Cells: At the Crossroads*', Progress in Photovoltaics: Research and Applications, Vol. 8, pp. 443 – 440, 2000.

[6] K. Shirasawa, '*Mass Production Technology for Multicrystaline of Solar Cells*', Progress in Photovoltaics: Research and Applications. Vol. 10, pp. 107 – 118, 2001.

[7] T. Jestre, '*Crystalline Silicon Manufacturing Progress*', Progress in Photovoltaics: Research and Applications, Vol. 10, pp. 99 - 106. 2002.

[8] M.A. Green, '*Third Photovoltaics Generation: Ultra-High Conversion Efficiency At Low Cost*', Progress in Photovoltaic: Research and Applications, Vol. 9, pp. 123 – 135, 2001.

[9] R.R. Arya and D.E. Carlson, '*Amorphous Silicon Statement Modulates Manufacturing At LP solar*', Progress in Photovoltaic: Research and Applications, Vol. 10, pp. 69 – 76, 2002.

[10] M.A.Green, K. Emery, D.L. King, S. Igari and W. Watra, '*Solar Cell Efficiency Tables (Version 19)*', Progress in Photovoltaic: Research and Applications, Vol. 10, pp. 55 – 61, 2002.

[11] H.J. Möller, '*Semiconductors for Solar Cells*', Artech House, Inc, Norwood, MA, 1993.

[12] J.P. Charles, A. Haddi, A. Maouad, H. Bakhtiar, A. Zerga, A. Hoffmann and P. Mialhe, '*The Junction, of Solar with Micro-Electronics*', Rev. Energ. Ren., Vol. 3, pp. 1 - 16, 2000.

[13] M.S. Imamura and J.I. Portscheller, '*Year Evaluation of the Methods of Determining Solar Cell Series Resistance*', Proceedings of 8^{ht} Photovoltaic Specialists Conf., Seattle, WA, pp. 102 - 107, 1970.

[14] H.J. Hovel, '*Semiconductors and Semimetals*', In 'Solar Cells', Vol. 11, Academic Press, New York, 1975.

[15] H. Knopf, '*Analysis, Simulation and Maximum of Evaluation Power Not Alignment (MPPT) Methods for Has Solar Powered Vehicle*', Master of Science in Electrical and Computer Engineering, Portland Cement State University, 1999.

[16] R.C. Neville, '*Solar Energy Conversion: The Solar Cell*', Vol. 1, Studies in Electrical and Electronic Engineering, Elsevier Scientific Publishing Company, N-Y, 1978.

[17] A.F. Boehinger, '*Coil-Adaptive cd. Converter for Solar Spacecraft Power Supply*', IEEE Transactions one Aerospace and Electronic Systems, AES -4, N°1, pp. 102 - 111, 1968.